



## Seismic Design and Response of a Gravity-Controlled Rocking Braced Frame System with Self-Centering Storey Shear Fuses

Simon Dufresne-Landry<sup>1\*</sup>, Robert Tremblay<sup>2</sup>

<sup>1</sup>M.Sc. Student, Civil Geological and Mining Eng. Dept., Student, Polytechnique Montréal, Montréal, QC, Canada

<sup>2</sup>Professor, Civil Geological and Mining Eng. Dept., Polytechnique Montréal, Montréal, QC, Canada

\*[simon.dufresne-landry@polymtl.ca](mailto:simon.dufresne-landry@polymtl.ca) (Corresponding Author)

### ABSTRACT

This paper describes a gravity-controlled rocking braced frame (G-CRBF) system that incorporates a self-centering (SC) storey shear fuses to control higher mode effects. An inverted-V bracing configuration is adopted for the system, and the SC storey shear fuses are obtained by implementing a friction connection designed to slip at predetermined loads in one of the two bracing members at every level. In the design methodology, three response spectrum analyses are performed to determine the seismic induced base overturning moment and axial loads in columns and bracing members from first mode and higher mode response. In one analysis, a flexible vertical spring is introduced at the base of one of the G-CRBF columns to simulate the conditions upon rocking. Brace axial loads from that analysis are reduced by a force modification factor  $R_{hm}$  to determine the slip load of the brace connections. The system is used for 12- and 16-storey office buildings located in Montreal, QC, and Vancouver, BC, to examine its applicability and seismic response for seismic conditions in eastern and western Canada. The seismic behaviour is investigated through nonlinear response history analyses (NLRHA) conducted with ensembles of site representative ground motion records using the SAP2000 computer program. Axial load demands on the G-CRBF members from NLRHA are compared to the design values. Peak and residual storey drifts, peak floor horizontal accelerations, peak brace connection slip displacements, and peak column uplifts from NLRHA are also presented to assess the performance of the system. The results show that the proposed G-CRBF system with SC storey shear fuses represents an effective means of controlling higher mode effects and improving the seismic performance of multi-storey steel building structures.

Keywords: Gravity-controlled rocking braced steel frames, Higher modes effects, Energy dissipation, Friction connections, beam flexure.

### INTRODUCTION

The use of controlled-rocking braced steel frames (CRBFs) for enhanced seismic performance of structures has been extensively researched experimentally and numerically over the last two decades [1-10]. In building structures, CRBFs are typically uncoupled from the gravity load carrying system such that column uplift can developed freely during strong seismic events, and self-centering response is achieved with vertical post-tensioned (PT) tendons that connect the column or beam at the roof level to the foundation. Energy-dissipating (ED) devices are also used between the column bases and the foundation to control lateral displacements upon rocking. In gravity-controlled rocking braced frames (G-CRBFs), the rocking frame is part of the building gravity load system and self-centering response is simply obtained by the gravity loads acting on the roof and floor beams supported by the frame [8-10]. PT elements and special detailing for vertically uncoupling the frame from the gravity system are then avoided. ED devices are still used at the column bases to control the rocking response.

Rocking braced steel frames are effective in limiting the base overturning moment and, thereby, column axial loads in the lower portion of the frames. However, the system is prone to the development of large storey shears due to elastic higher mode response that takes place upon rocking at the base that can induces high axial loads in beams and bracing members over the frame height as well as large column axial loads in the upper levels. Methods have been proposed to predict that force demand [13, 14]. However, accounting for those additional force demand in design detrimentally impacts the cost-effectiveness of CRBFs. The introduction of a nonlinear self-centering (SC) storey shear fuse at the structure base has been proposed to control storey shears and improve the cost-efficiency of the system. However, the benefits were limited to the bottom structure levels.

In a more recent study [15], it was shown that higher mode response could be reduced uniformly over the entire height of G-CRBFs by introducing self-centering (SC) shear fuses at every building level [15]. The shear fuses are obtained by means of bolted connections that are detailed to slip at predetermined loads in one of the two inverted-V bracing members. Storey shears are therefore limited by the slip resistance of the brace connections. The beams are designed to deform elastically in bending under the vertical resultant of the unbalanced brace forces that develop upon slippage of the brace connections, which provides self-centering response for the storey shear fuses.

This preliminary investigation on G-CRBFs with distributed storey shear fuses was performed for 4-, 8-, and 12-storey buildings located in Vancouver, BC, and the structures were designed using the seismic data of the 2015 edition of the NBC. In the 2020 NBC, the seismic hazard in Southwest British Columbia has been increased markedly and it was felt necessary to verify that the proposed G-CRBF system could still perform adequately under more severe seismic conditions. Moreover, there was an interest in examining the applicability of the system for taller structures and for structures subjected to ground motions records compatible with the seismic hazard of eastern Canada. This article presents a study on the use of the system for 12- and 16-storey buildings located in Vancouver, BC, for western Canada, and Montreal, QC, for eastern Canada.

The analysis and design procedure for sizing the members of G-CRBFs, including the elements forming the SC storey shear fuses, is first presented. The seismic response of the G-CRBF structures is then examined by means of nonlinear response history analyses performed under ensembles of site representative ground motion records. The response parameters investigated include the peak and residual storey drifts, peak horizontal floor acceleration, peak slip displacements in brace connections, peak uplift at the column bases, and peak axial load demands in the G-CRBF members.

## STRUCTURES STUDIED

### Configuration

Detail of the structures studied is presented in Figure 1. As shown, two G-CRBFs were used in each of the two orthogonal directions for the 12-storey buildings. For the 16-storey structures, four braced frames in each direction were required to properly control storey drifts. The structures consist of a central core bay surrounded by office space. In this article, the response of the structures along the E-W direction is examined.

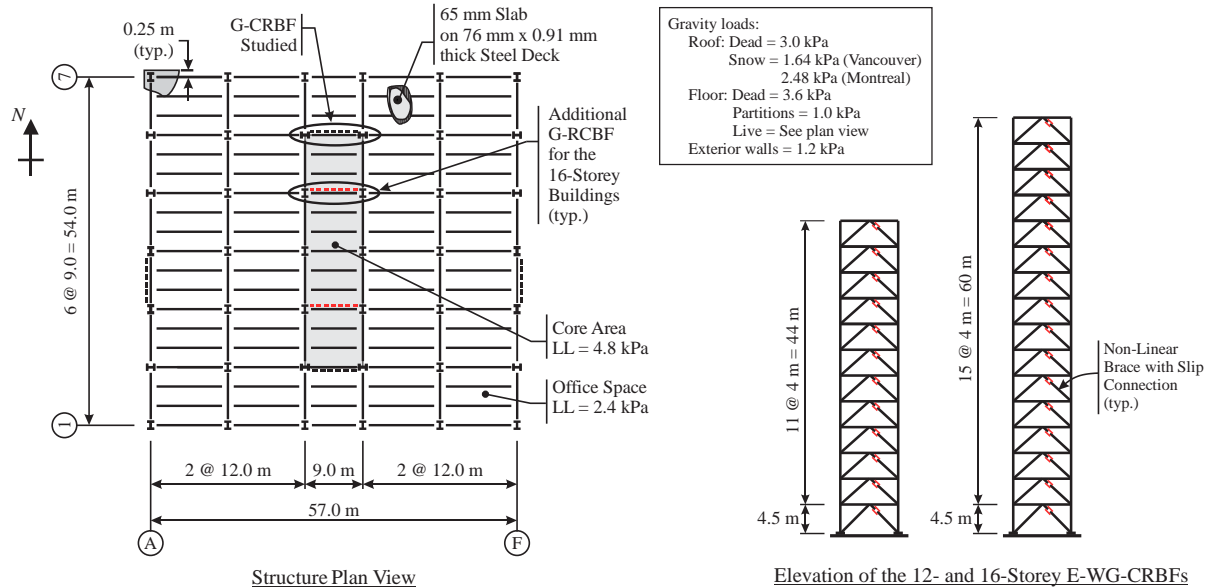


Figure 1. Studied Structures

### G-CRBF design

The design of the system was performed in accordance with the provisions of the 2020 NBC [14] and the steel design standard CSA S16-19 [15]. Members forces from the most critical of the seismic load combinations including dead loads only ( $D + E$ ) and dead loads plus concomitant live and snow loads ( $D + 0.5 L + 0.25 S + E$ ) were considered. Column and beam members are made of ASTM A992 W shapes whereas ASTM 1085 HSS profiles are used for the bracing members. As illustrated in Figure 2, seismic induced member forces were determined using three response spectrum analyses (RSA) conducted on different frame models with different design spectra.

The first RSA was conducted on a fixed base frame model to obtain the base vertical reaction due to the seismic overturning moment,  $R_E$ . In this analysis, the results were adjusted such that the base shear from the analysis was equal to the specified lateral earthquake load from the NBC,  $V_{NBC}$ , calculated with a ductility-related force modification factor,  $R_d$ , equal to 8.0, and an overstrength-related factor  $R_o$  equal to 1.0. The resulting seismic effects then approximately corresponded to those that would be determined for the most ductile seismic force resisting systems currently specified in the NBC. The frictional resistance of the ED devices at the column base,  $F_R$ , was then obtained from:  $F_R = R_E - R_D$ , where  $R_D$  is the vertical reaction from gravity dead loads. The second RSA was performed with consideration of the first mode properties only to obtain member axial loads from the building first mode response prior to rocking. The results of this analysis were adjusted such that the vertical reaction at the frame base,  $R_E$ , was same as the one obtained from the first RSA. In the third RSA, a flexible spring was introduced at the base of one column to simulate the base support conditions upon rocking. For this analysis, the design spectrum was reduced by a higher mode response force modification factor,  $R_{hm}$ , also set equal to 8.0. The spectrum was also truncated for periods beyond the first mode period to isolate member forces from higher mode response upon rocking.

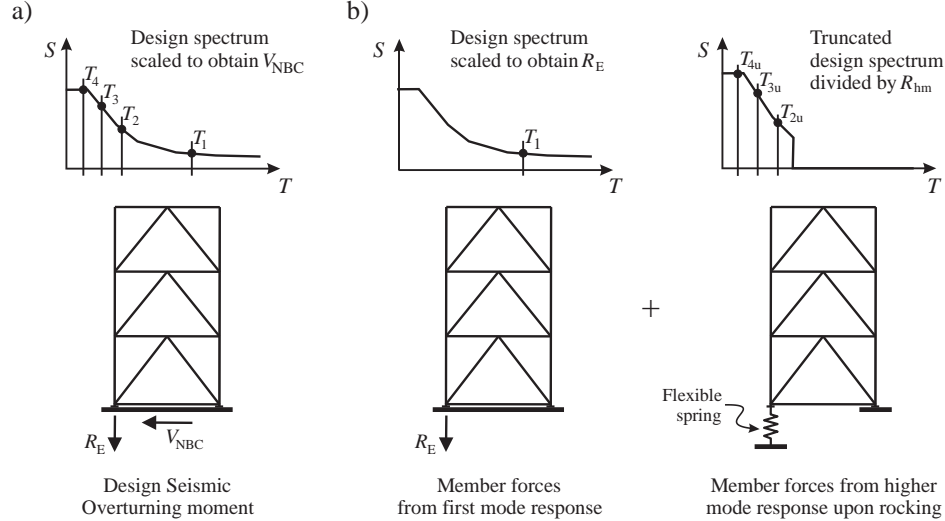


Figure 2. Response spectrum analyses (RSA) using: a) Fixed base frame model; b) Fixed base frame model considering first-mode contribution only; and c) Frame model with a flexible base spring and a reduced and truncated spectrum.

Axial loads for the bracing and column members as obtained from the analyses are presented in Figure 3. Forces from the second RSA are first combined with those from dead load plus concomitant live and roof snow loads ( $0.5 L + 0.25 S$ ). Axial loads from the third RSA are then added to obtain the total loads used in design. Total loads are given for  $R_{hm} = 1$  and  $R_{hm} = 8$  to illustrate the significant reduction in higher mode induced member forces that results from introducing the storey shear fuses along the frame height compared to the force demand from higher modes that would need to be considered for the same CRBFs without storey shear fuses. Column sections were selected to resist the total axial compression shown in Figure 3, plus the additional load  $P_c$  describes below. For the non-linear braces with friction connections, the slip resistance of the connections  $F_{ds}$  was set equal to the total brace axial loads determined with  $R_{hm} = 8$ . HSS profiles for the nonlinear braces were then selected to resist compressive loads equal to  $F_{ds}$ .

The storey shear-storey drift response of the proposed G-CRBF system is described in Figure 4. In the figure, the storey drift is the one due to storey shear only and does not include the storey drift due to overall flexural response of the frame. As shown, once brace connection slip has occurred, the storey shear stiffness reduces to  $k'_s$  governed by the axial stiffness of the linear brace (brace without friction connection) and the axial and flexural stiffness properties of the beam:

$$k'_s = \frac{V'}{\Delta'} = \frac{1}{\left( \frac{L}{2EA_b} + \frac{L}{EA_d \cos^3 \theta} + \frac{L^3 \tan^2 \theta}{48EI_b} \right)}, \text{ for } \Delta_{slip} < \Delta < \Delta_m \quad (1)$$

The HSS profiles for the linear braces and the W shapes for the beams were selected to obtain a stiffness  $k'_s$  equal to or greater than 1.5 times the negative storey shear stiffness due to P-delta effects induced by the total compression load  $\Sigma C_f$  carried by the building columns laterally stabilized by each G-CRBF,  $\Sigma C_f/h_s$ , so that the frame exhibits a net positive storey shear stiffness upon slippage of the brace friction connections to provide self-centering capacity to the storey shear fuses. The beams and linear braces were also selected to resist member forces anticipated at a target storey drift  $\Delta_t$  which was set equal to 1.5%  $h_s$  in this study. The storey shear  $V_t$  required to reach  $\Delta_t$  is determined from Eq. (2) with the stiffness  $k'_s$  and the storey shear and drift at brace connection slip,  $V_{slip}$  and  $\Delta_{slip}$ , as obtained from Eq. (3). For the beams, Eq. (4) is used to verify that the selected section can resist the combined axial compression load and bending moment induced by the storey shear  $V_t$ . In Eq. (4),  $M_{b,grav}$

is the bending moment from gravity loads on the beam, and  $P_{y,b}$  and  $M_{p,b}$  are the yield axial and flexural resistances of the beam calculated with the probable yield stress,  $R_y F_y$ . The linear braces must have a factored axial compressive resistance equal to or greater than the load  $F_{dt}$  given by Eq. (5). At the target drift, the vertical resultant of the unbalanced brace loads causing bending of the beams also induces additional compression loads  $P_c$  in the columns, as given in Eq. (5). The selected column sections must then be adjusted as necessary to ensure that they can resist those additional loads. The computed periods in the first three modes of vibration of the structures are given in Table 1. The steel tonnage required for the proposed G-CRBFs are given in Table 2. For comparison purposes, the design was also performed using loads obtained with  $R_{hm} = 1$ , which would represent the case of a G-CRBF without SC shear fuses. As shown, the use of the SC storey shear fuses led to reduction in steel varying from 20 to 23%, which can positively impact on construction costs and sustainability.

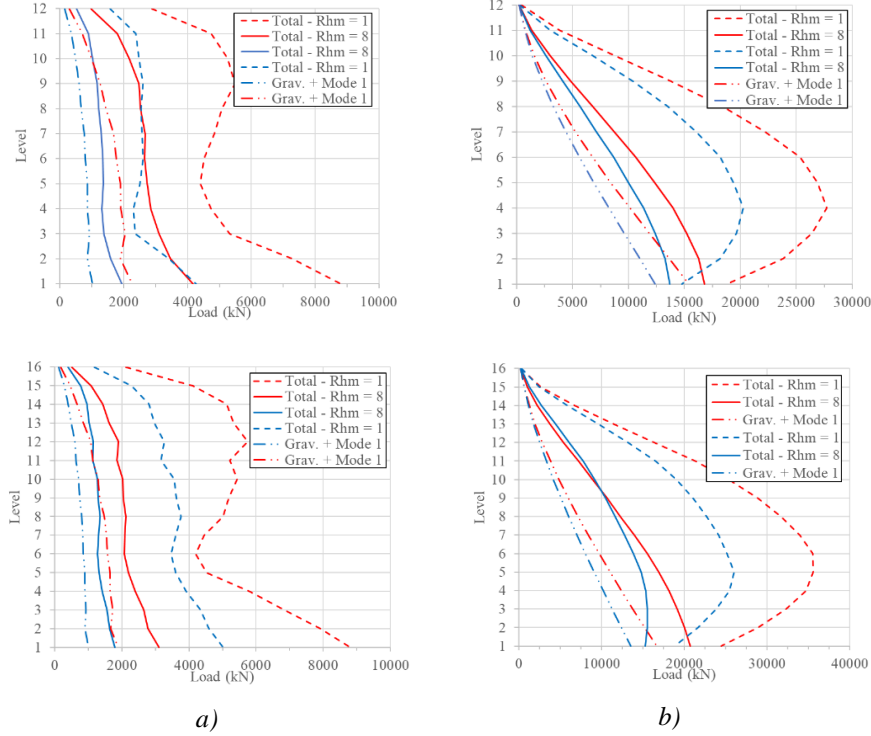


Figure 3. Axial loads from gravity loads and response spectrum analyses in: a) Bracing members; and b) Columns. (note: blue lines = Montreal; red lines = Vancouver).

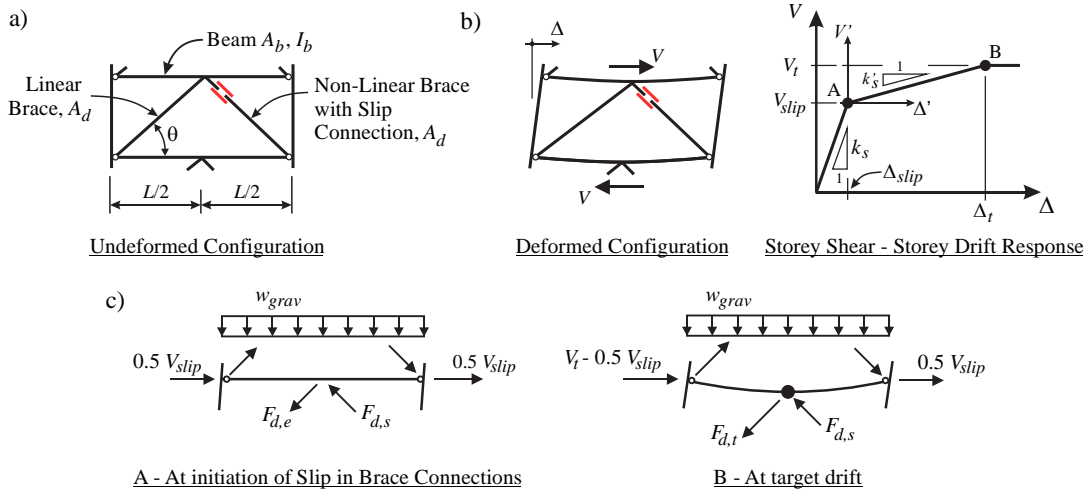


Figure 4. Response of G-CRBF with SC shear fuses under storey shear: a) Frame geometry; b) Storey shear vs storey drift response; c) Conditions at initiation of slip in brace connections and at beam yielding.

$$V_t = k'_s (\Delta_t - \Delta_{slip}) + V_{slip} \quad (2)$$

$$V_{slip} = 2F_{ds} \cos \theta + \frac{0.625 w_{grav} L}{\tan \theta}; \Delta_{slip} = \frac{V_{slip}}{k_s}; \frac{1}{k_s} = \frac{L}{4EA_b} + \frac{L}{4EA_d \cos^3 \theta} \quad (3)$$

$$V_t = V_{slip} + \min \left[ \frac{M_{pb} - M_{b,grav}}{\tan \theta \left( \frac{L}{4} \right)}; \frac{P_{yb} - 0.5 V_{slip} - 0.85 M_{b,grav} \left( \frac{P_{yb}}{M_{pb}} \right)}{1 + 0.85 \tan \theta \left( \frac{L}{4} \right) \left( \frac{P_{yb}}{M_{pb}} \right)} \right] \quad (4)$$

$$F_{dt} = \frac{V_t - 0.5 V_{slip}}{\cos \theta}; P_c = \frac{V_t - V_{slip}}{2 \tan \theta} \quad (5)$$

Table 1. Fixed base periods of the structures studied.

Location		$T_1$ (s)	$T_2$ (s)	$T_3$ (s)
Montreal	12-storey	4.18	1.34	0.69
	16-storey	4.67	1.42	0.74
Vancouver	12-storey	3.62	1.10	0.58
	16-storey	4.13	1.25	0.63

Table 2. Required steel tonnage for the studied G-CRBFs.

Location		With no SC fuses ( $R_{hm} = 1$ ) (t)	With SC fuses ( $R_{hm} = 8$ ) (t)	Reduction (%)
Montreal	12-storey	81.5	65.5	21
	16-storey	115.8	92.2	23
Vancouver	12-storey	92.9	78.0	18
	16-storey	118.9	97.6	20

## NONLINEAR RESPONSE HISTORY ANALYSIS

Nonlinear response history analysis (NLRHA) was performed to validate the proposed design method and examine the seismic response of the structures studied. For Vancouver, the structures were subjected to two suites of site representative ground motion records: a first suite that comprised 6 records from crustal (CR) EQs plus 5 records from deep in-slab subduction (IS) EQs, and a second suite of 11 records from subduction interface (IF) EQs. For the Montreal site, only one suite of 11 ground motion records was used that included 3 records from small earthquakes at short distances and 8 records from larger earthquakes at longer distances. As illustrated in Figure 5, the ground motion records were scaled to the UHS at the sites in accordance with the guidelines of Commentary I of NBC 2020.

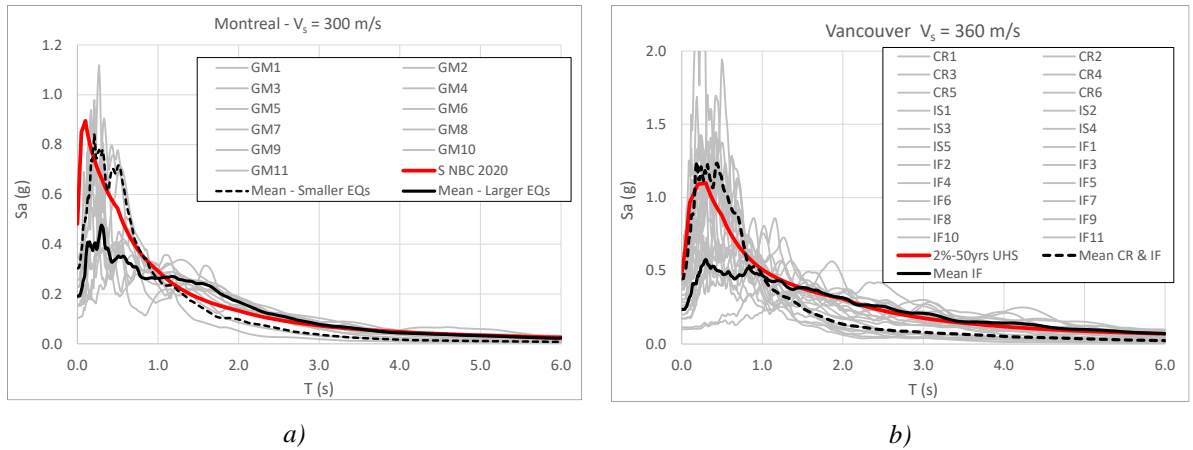


Figure 5. 5% damped acceleration spectra of the ground motion records for: a) Montreal; and b) Vancouver.

NLRHA was conducted using the SAP2000 structural analysis software [18]. As shown in Figure 6, the model included half the building structure. The non-linear braces with friction connections were modelled using nonlinear link elements which were assigned a stiffness equal to the axial stiffness of the braces and a plastic Wen hysteresis to simulate the slip response of the

connections. Nonlinear link gap elements were used at the column bases to reproduce stiff contact conditions under compression and free column uplift. Nonlinear link elements with plastic Wen hysteresis were also introduced at the column bases to simulate the ED devices. In the analyses, Rayleigh damping corresponding to 3% of critical damping in modes 1 and 3 of the fixed base structures was considered. Stiffness proportional damping was only assigned to the steel material to avoid spurious damping forces in the nonlinear link elements. Gravity loads corresponding to  $D + 0.5L + 0.25S$  was applied on the form of distributed masses assigned to the floor and roof beams. In NLHRA, the structure was subjected to a constant vertical acceleration of 1.0 g together with the horizontal ground motion records to include the dynamic vertical response of the G-CRBF and adjacent gravity framing members resulting from uplifting of the G-CRBF columns.

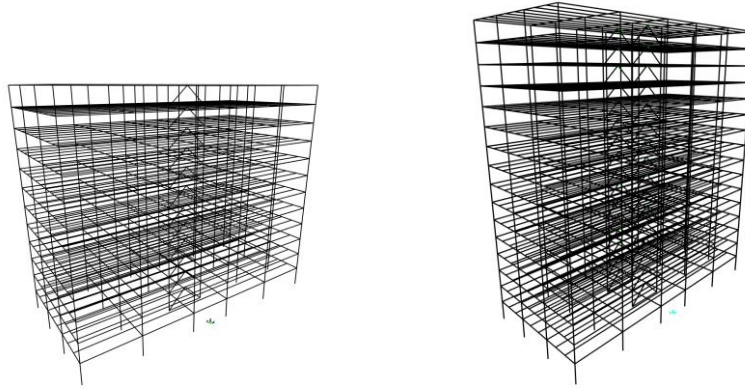


Figure 6. SAP2000 models used for NLRHA of the 12-storey (left) and 16-storey (right) G-CRBFs.

## Results

The response parameters that are examined herein are the peak and residual storey drifts, peak horizontal floor accelerations, peak axial loads in the bracing and column members, slip displacements in the brace connections, and column vertical uplift displacements.

Typical time history response of the first-storey drift and roof drift are presented in Figure 7 for the 12-storey G-CRBF in Vancouver under a crustal EQ ground motion record and an interface subduction EQ ground motion record. As shown, the structure response is dominated by first mode response as both drift responses are in phase and have comparable amplitudes. Under both ground motions, the structure oscillated about its undeformed position over the duration of the ground motions and did not sustain significant residual lateral deformations at the end of the seismic events.

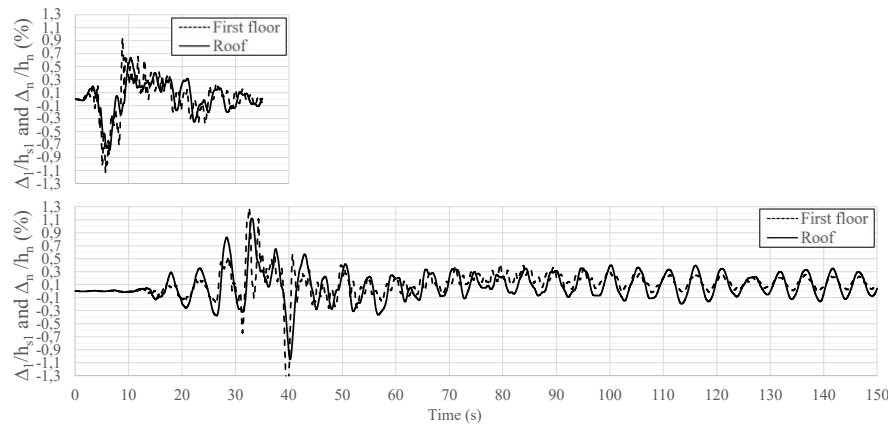


Figure 7. Roof and storey drift histories of the 12-storey G-CRBF in Vancouver under the 1994 M6.7 Northridge EQ, St. Sun Valley - Roscoe Blvd 0° record (top) and the 2003 M8.3 Tokachi-oki, Japan, St. Kuriyama N-S record (bottom).

Peak storey drift results are presented in Figure 8. As shown, mean peak storey drifts for the two structures in Montreal are approximately equal to  $0.5\% h_s$  over the entire building height. The structures in Vancouver also experienced mean peak storey drifts of  $0.5\% h_s$  under the crustal and in-slab EQ ground motions, and approximately  $1\% h_s$  under the interface subduction ground motions. These results show that the system can be used at both locations to obtain peak storey drifts under design level ground motions that meet the NBC  $1.0\% h_s$  limit for post-disaster buildings and that are well below the  $2.5\% h_s$  for buildings of the normal importance category. The results also show that, at both locations, the 16-storey buildings with four G-CRBFs in



the E-W direction sustained smaller storey drifts compared to the 12-storey ones designed with two G-CRBFs in the E-W direction. The better drift performance of the 16-storey building is attributed to the relatively higher self-centering capacity that could be achieved with the larger number of G-CRBFs. In the figure, it can also be noted that peak negative storey drifts towards the West are slightly larger than the positive ones. This asymmetry is attributed to the shakedown response of the beams under gravity loads that leads to progressively accumulated downward beam deflections upon slippage of the nonlinear brace friction connections which, in turn, results in positive storey drifts.

Residual deformation response of the structures was studied by examining at the roof drifts  $\Delta_n/h_n$  at the end of the ground motions. For the 12- and 16-storey buildings in Montreal, the mean and maximum values among the 11 records are respectively equal to 0.21 and 0.25 %. For the structures in Vancouver, the corresponding values are 0.23% and 0.28%. It is noted that the results did not significantly differ between the 12 and 16-storey structures. These low values can be attributed to the system's recentring capabilities, as shown in Figure . The results suggest that gravity recentring is effective in controlling excessive permanent displacement at all levels of the building, and that first mode response dominate the structure deformation.

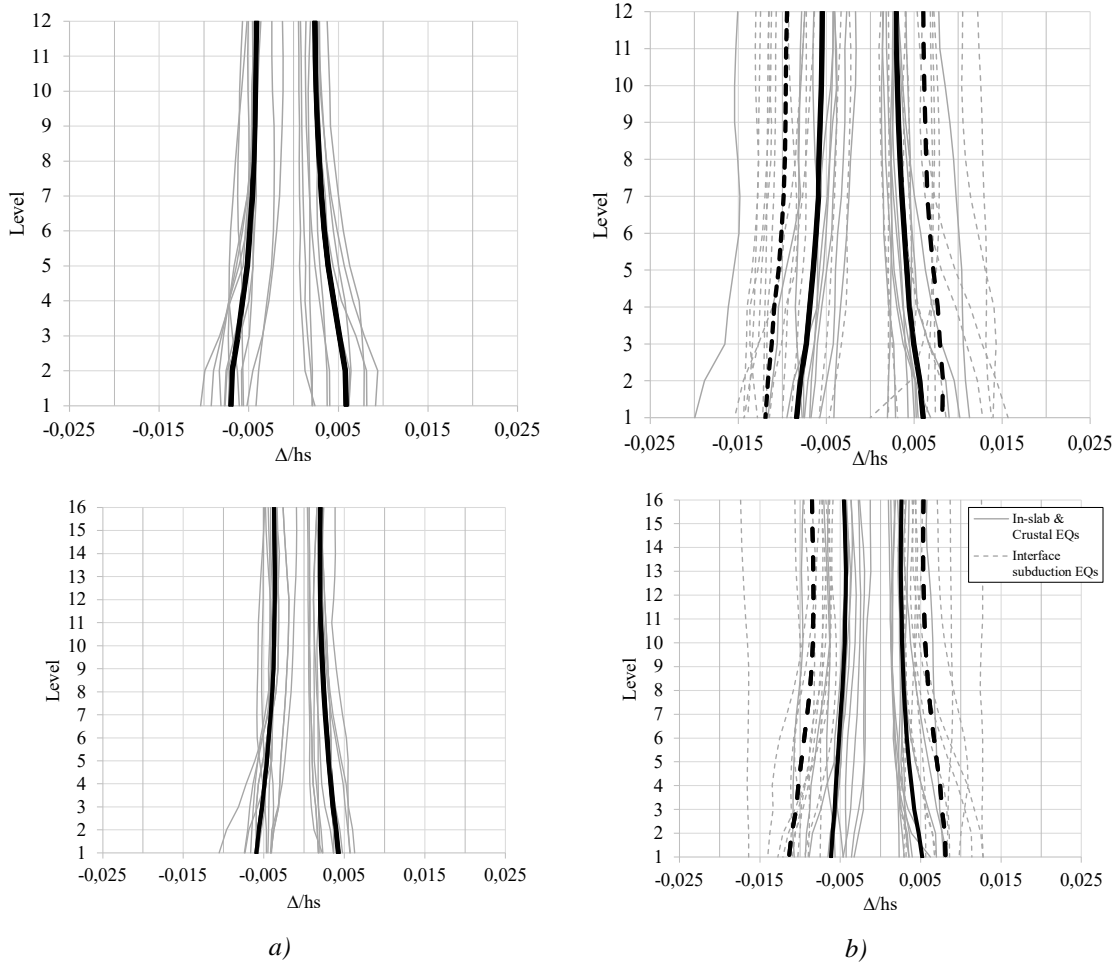


Figure 8. Peak storey drifts in: a) Montreal; b) Vancouver.

Peak floor horizontal acceleration results are presented in Figure 9. As shown, floor accelerations remained below 1 g in all cases, with maximum peak values of 0.93g and 0.47 g for Vancouver and Montreal, respectively. For the structures in Vancouver, it is observed that the interface subduction EQ ground motions induced lower floor accelerations compared to the ground motions from crustal and in-slab EQs, which can be attributed to the longer dominant periods of the interface subduction records. The figure also shows that floor accelerations can be effectively controlled over the full height of the buildings, regardless of the location and number of storeys of the buildings. This behaviour is the result of the storey shear fuses limiting storey shears and dissipating energy through friction at every level of the structures. Such a response indicate that the system can provide adequate protection for acceleration-sensitive building content and equipment, even in a 16-storey structure. This is different from conventional CRBFs which typically sustain high accelerations near the roof level or increasing accelerations when the number of storeys is increased.

Mean values of the peak axial load demands in the bracing members and columns from NLRHA are presented in Figure 10 for the Montreal and Vancouver buildings. The values adopted in design are also presented in the plots. For the structures at both locations, maximum compression and tension axial loads in the braces were well predicted with the RSA performed in the design phase, except in the lower levels of the structures in Vancouver where the compression loads imposed by the interface subduction EQ ground motions slightly exceeded the design values. The figure also shows that the brace force demands in the 16-storey buildings are generally lower than that of the 12-storey structures, which confirms the effectiveness of the storey shear fuses in limiting storey shears from higher mode response. Column axial loads were well predicted for both buildings in Montreal, except in the first level of the 16-storey building. For the buildings in Vancouver, column loads used in design matched well or exceeded the force demands from crustal and in-slab EQ ground motions but the ground motions from interface subduction EQ ground motions exceeded the design predictions in the lower half of the two buildings. The relatively larger axial load demand in braces and columns from interface subduction EQ ground motions can be attributed to a higher than predicted building first mode response under those ground motions characterized by longer dominant periods.

To examine further the efficiency of the storey shear fuses in limiting member forces, NLRHA was repeated for the G-CRBFs designed with  $R_{hm} = 1.0$  for the 12- and 16-storey buildings in Montreal. Mean axial load demands in bracing members and columns for the G-CRBFs with SC shear fuses ( $R_{hm} = 8$ ) are compared to those for the G-CRBFs without SC shear fuses ( $R_{hm} = 1.0$ ) in Figure 11. As shown, the use of the storey shear fuses contributed to reduce considerably member forces over the entire height of the frames. For the bracing members, larger reductions are observed at the base and in the upper half of the frame height, where large storey shears from higher modes typically develop in multi-storey buildings. For the columns, the reduction is more pronounced near in the middle third of the frame height, where overall bending from higher modes is the largest in conventional CRBFs.

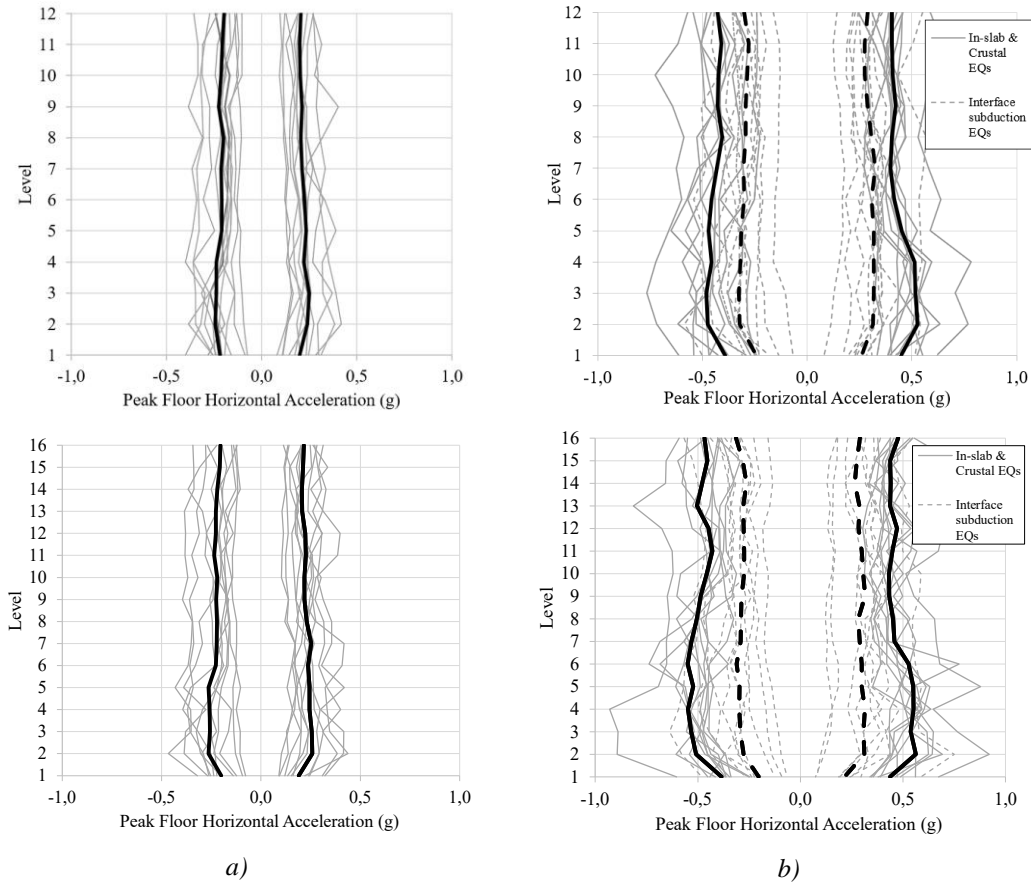


Figure 9. Peak floor accelerations in: a) Montreal; b) Vancouver.



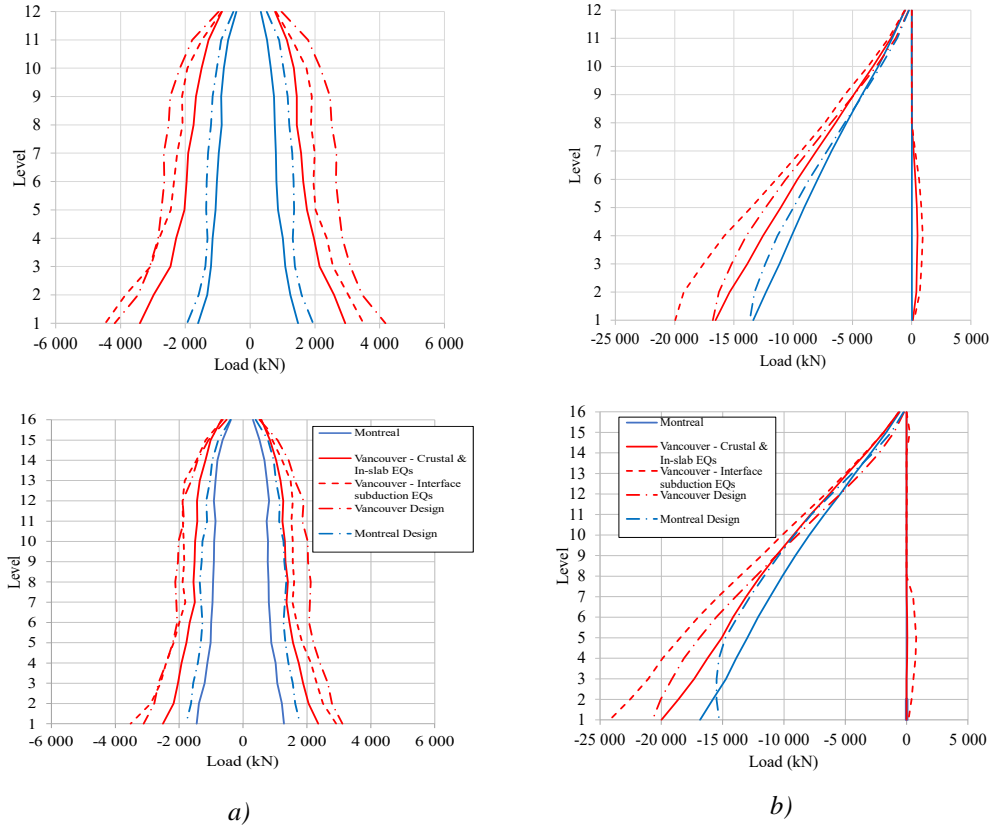


Figure 10. Mean Peak axial load demands in: a) Bracing members; and b) Columns.  
(Note: blue lines = Montreal; red lines – Vancouver)

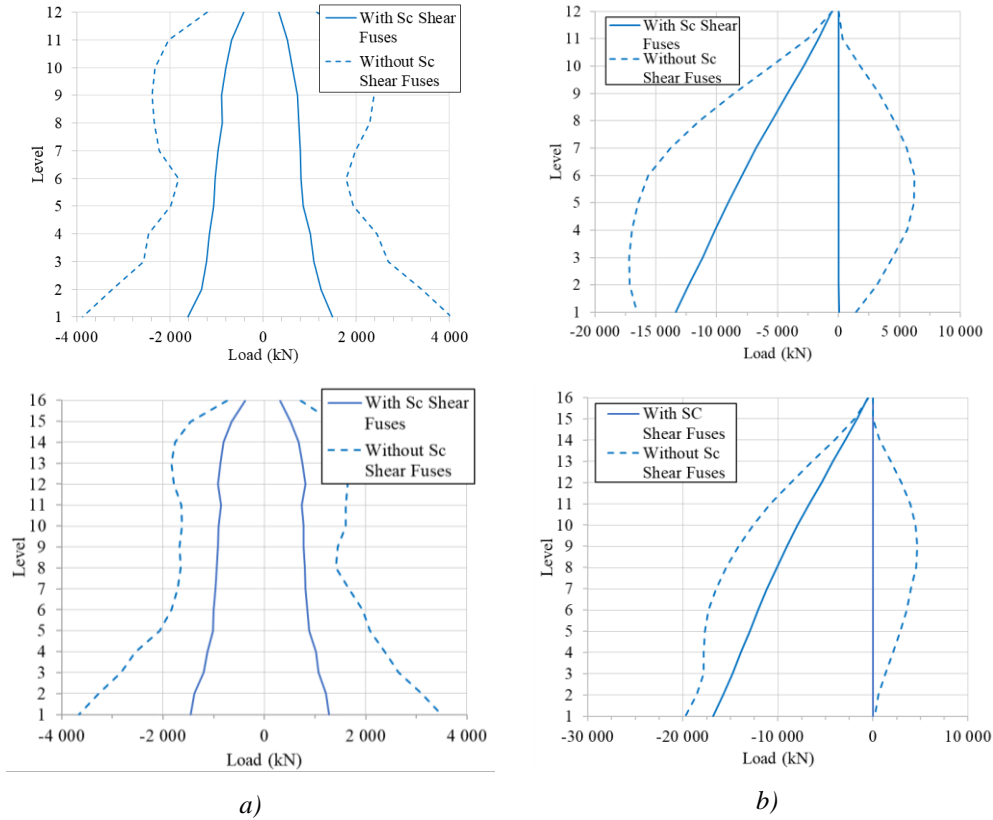


Figure 11. Comparison of mean peak axial loads with and without SC shear fuses in: a) Bracing members; and b) Columns.

To verify the feasibility of the proposed G-CRBF system with storey shear fuses, the amplitude of slip displacements experienced in the friction brace connections were examined together with the amplitude of column base uplift excursions. The mean values of peak slip displacements are presented in Figure 12 for the four buildings. As shown, slip demands on the connections of the G-CRBFs in Montreal compare well with the slip demands from the crustal and in-slab EQ ground motions of the frames in Vancouver. For the latter, however, interface subduction EQ ground motions imposed larger slip displacements, especially for the 12-storey building. Overall, mean slip displacements remained reasonable, however, ranging from 10 mm to 43 mm, which can be easily accommodated with simple bolted connections with slotted holes.

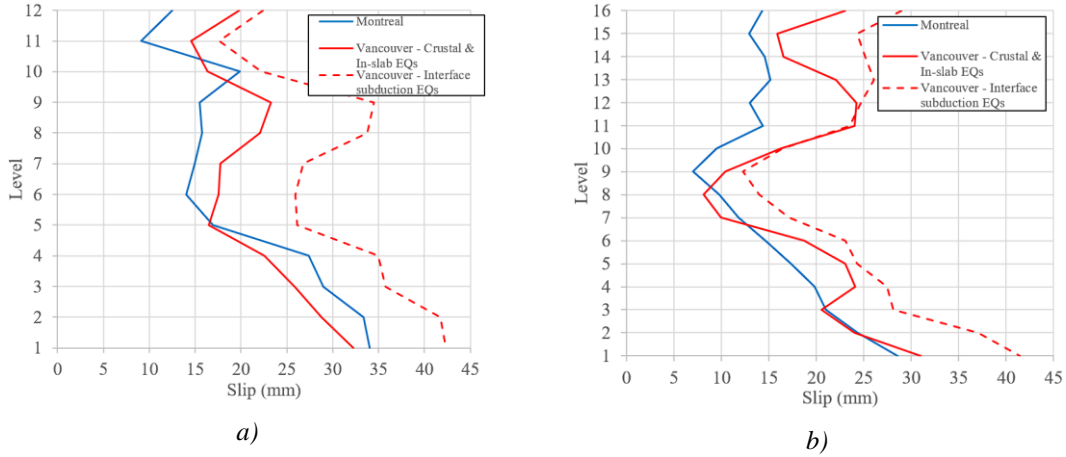


Figure 12. Mean peak values of brace connection slip in the: a) 12-storey G-CRBFs; and b) 16-storey G-CRBFs.

In Figure 13, time history of the roof drift, axial loads, and column base uplift are plotted for a 60 s time window corresponding to the strong motion portion of an interface subduction ground motion. These results again confirm that G-CRBF response under strong ground shaking is dominated by first mode and base rocking. In that case, the roof drifts reached 1.0 % and 1.5 % of the building height towards the East and West directions, respectively. In the half-cycle with 1.5%  $h_n$  roof displacement towards the West, the East column uplifted by approximately 110 mm. This corresponds to a base rocking angle of approximately 0.012 rad. ( $\approx 110/9300$ ), which is consistent with the observed 1.5% roof drift when considering the additional roof drift induced by the global flexural deformations of the frame over its height. Statistics of column uplift amplitudes are given in Table 3. Again, the values are reasonable and can be accommodated with simple friction base ED devices.

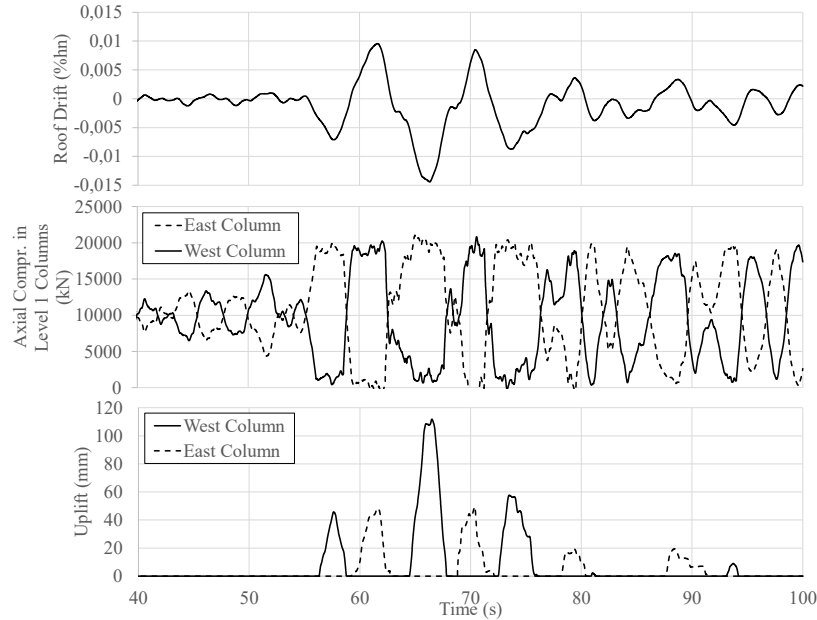


Figure 13. Time history of the roof drift, column axial compression load and column base uplift of the 12-storey G-CRBF in Vancouver during the strong motion portion of the under the 2003 M8.3 Tokachi-oki, Biratori-W, EW record:  
a) Roof drift; b) Column axial load, and c) Column uplift.

Table 3. Peak column uplift.

Location	Height	EQ source	Range (mm)	Mean value (mm)
Montreal	12-storey	-	47-63	57
	16-storey	-	28-44	38
Vancouver	12-storey	Crustal & Inslab	86-92	87
		Interface Subduction	96-114	109
	16-storey	Crustal & Inslab	67-77	73
		Interface Subduction	71-88	85

## CONCLUSIONS

This article presented a steel gravity-controlled rocking braced frame (G-CRBF) system in which self-centering storey shear fuses are introduced at every level to reduce higher mode response. An inverted-V bracing configuration is used and the storey shear fuses are obtained by having a bolted connection designed to slip at predetermined load at the end of one of the bracing members to limit storey shear and dissipate energy through friction. Upon slippage of the brace connection in a level, the second bracing member acts in series with the beam in flexure to develop an elastic storey shear-storey drift response, which provides self-centering capacity for the shear fuse. A design procedure was presented that involves three response spectrum analyses to obtain member forces up to initiation of rocking and additional member forces due to higher mode response upon rocking. A design method to achieve the intended self-centering response for the shear fuse was also presented.

The seismic response of the proposed G-CRBF system and the adequacy of the proposed design methodology was verified for 12- and 16-storey office buildings located in Montreal, QC, for eastern Canada, and Vancouver, BC, for western Canada. The application of the design procedure was illustrated for the building studied. It was shown that the storey shear fuses can reduce significantly member forces due to higher mode response compared to the same frames designed without the shear fuses. Nonlinear response analyses were then conducted using site representative ensembles of ground motion records to investigate the seismic response of the structures and validate the member forces predicted for design. The results showed that the system can lead to limited and uniform peak storey drifts and peak floor accelerations over the entire frame building, confirming its efficiency in controlling higher mode response.

This preliminary study shows that the system has strong potential for achieving superior seismic performance of building structures and improve the seismic resilience of cities located in active seismic zones. Additional studies are needed to further investigate the behaviour of the system for other applications such as taller buildings, buildings on other soil conditions or located in regions subjected to different seismic hazard.

## ACKNOWLEDGMENTS

Funding was provided by the Natural Science and Engineering Research Council of Canada (NSERC).

## REFERENCES

- [1] Zhong, C., and Christopoulos, C. (2022). "Self-centering seismic-resistant structures: Historical overview and state-of-the-art," *Earthquake Spectra*, 38(2), 1321-1356.
- [2] Midorikawa, M., Azuhata, T., Ishihara, T., and Wada, A. (2006) "Shaking table tests on seismic response of steel braced frames with column uplift," *Earthquake Engng & Struct. Dyn.*, 35(14), 1767-1785.
- [3] Pollino, M., and Bruneau, M. (2007). "Seismic Retrofit of Bridge Steel Truss Piers Using a Controlled Rocking Approach," *J. Bridge Eng.*, ASCE, 12(5), 600-610.
- [4] Tremblay, R., Poirier, I.-P., Bouaanani, N., Leclerc, M., René, V., Fronteddu, L., and Rivest, S. (2008). "Innovative viscously damped rocking braced steel frames," *Proc. 14<sup>th</sup> World Conf. on Earthquake Eng.*, Beijing, China, Paper no. 14-05-01-0527.
- [5] Sause, R., Ricles, J.M., Roke, D.A., Chancellor, N.B., and Gonner, N.P. (2010). "Seismic performance of a self-centring rocking concentrically-braced frame," *Proc. 9<sup>th</sup> US Nat. and 10<sup>th</sup> Can. Conf. on Earthquake Eng.*, Toronto, Canada, Paper No. 1330.
- [6] Eatherton, M.R., Ma, X., Krawinkler, H., Mar, D., Billington, S., Hajjar, J.F., and Deierlein, G., (2014). "Design Concepts for Controlled Rocking of Self-Centering Steel-Braced Frames," *J. Struct. Eng.*, ASCE, 140(11).

- [7] Pollino, M. (2015). "Seismic design for enhanced building performance using rocking steel braced frames," *Eng. Struct.*, 83, 129-139.
- [8] Mottier, P., Tremblay, R., and Rogers, C. (2018). "Seismic retrofit of low-rise steel buildings in Canada using rocking steel braced frames," *Earthquake Engng. & Struct. Dyn.*, 47, 333-355.
- [9] Mottier, P., Tremblay, R., and Rogers, C. (2021). "Shake table test of a two-story steel building seismically retrofitted using gravity-controlled rocking braced frame system," *Earthquake Engng. & Struct. Dyn.*, 50(6), 1576-1594.
- [10] Mottier, P., Tremblay, R., and Rogers, C. (2021). "Seismic behaviour of multi-storey gravity-controlled rocking braced-frame buildings including floor vertical response," *J. Constr. Steel Res.* 182.
- [11] Wiebe, L., Christopoulos, C., Tremblay, R., and Leclerc, M. (2013). "Mechanisms to limit higher mode effects in a controlled rocking steel frame. 1: Concept, modelling, and low-amplitude shake table testing," *Earthquake Engng. & Struct. Dyn.*, 42(7), 1053-1068.
- [12] Wiebe, L., Christopoulos, C., Tremblay, R., and Leclerc, M. (2013). "Mechanisms to limit higher mode effects in a controlled rocking steel frame. 2: Large-amplitude shake table testing," *Earthquake Engng. & Struct. Dyn.*, 42(7), 1069-1086.
- [13] Wiebe, L., and Christopoulos, C. (2015). "Performance-Based Seismic Design of Controlled Rocking Steel Braced Frames. II: Design of Capacity-Protected Elements," *J. Struct. Eng.*, ASCE, 141(9).
- [14] Martin, A., Deierlein, G.G., and Ma, X. (2019). "Capacity Design Procedure for Rocking Braced Frames Using Modified Modal Superposition Method," *J. Struct. Eng.*, ASCE, 145(6).
- [15] Tremblay, and Mottier, P. (2021). "A simple self-centering shear fuse for cost-effective controlled rocking steel braced frames," *Proc. 17th World Conf. on Earthquake Eng.*, Sendai, Japan, Paper no. C002427.
- [16] Canadian Commission on Building and Fire Codes - CCBFC (2022). *National Building Code of Canada 2020*. Prepared by the CCBFC, National Research Council of Canada, Ottawa, ON.
- [17] Canadian Standard Association – CSA (2019). *CAN/CSA-S16: Design of Steel Structures*. Prepared by the CSA, Toronto, ON.
- [18] Computers & Structures, Inc. (2023). *SAP2000 Ultimate, v23.2.0*, Computers & Structures, Inc., Walnut Creek, CA, USA.